Featured in Physics

Structure and equation of state of $Bi_2Sr_2Ca_{n-1}Cu_nO_{2n+4+\delta}$ from x-ray diffraction to megabar pressures

Alexander C. Mark,[1] Muhtar Ahart,[1] Ravhi Kumar,[1] Changyong Park,[2] Yue Meng,[2] Dmitry Popov,[2] Liangzi Deng,[3] Ching-Wu Chu,[3] Juan Carlos Campuzano,[1] and Russell J. Hemley[4]

[1]*Department of Physics, University of Illinois Chicago, Chicago, Illinois 60607, USA*

[2]*HPCAT, X-ray Science Division, Argonne National Laboratory, Lemont, Illinois 60439, USA*

[3]*Department of Physics and Texas Center for Superconductivity, University of Houston, Houston, Texas 77204, USA*

[4]*Departments of Physics, Chemistry, and Earth and Environmental Sciences, University of Illinois Chicago, Chicago, Illinois 60607, USA*

(Received 15 December 2022; accepted 5 May 2023; published 14 June 2023)

Pressure is a unique tuning parameter for probing the properties of materials, and it has been particularly useful for studies of electronic materials such as high-temperature cuprate superconductors. Here we report the effects of quasihydrostatic compression produced by a neon pressure medium on the structures of bismuth-based high-T_c cuprate superconductors with the nominal composition $Bi_2Sr_2Ca_{n-1}Cu_nO_{2n+4+\delta}$ ($n = 1, 2, 3$) up to 155 GPa. The structures of all three compositions obtained by synchrotron x-ray diffraction can be described as pseudotetragonal over the entire pressure range studied. We show that previously reported pressure-induced distortions and structural changes arise from the large strains that can be induced in these layered materials by nonhydrostatic stresses. The pressure-volume equations of state (EOS) measured under these quasihydrostatic conditions cannot be fit to single phenomenological formulation over the pressure ranges studied, starting below 20 GPa. This intrinsic anomalous compression as well as the sensitivity of $Bi_2Sr_2Ca_{n-1}Cu_nO_{2n+4+\delta}$ to deviatoric stresses provide explanations for the numerous inconsistencies in reported EOS parameters for these materials. We conclude that the anomalous compressional behavior of all three compositions is a manifestation of the changes in electronic properties that are also responsible for the remarkable nonmonotonic dependence of T_c with pressure, including the increase in T_c at the highest pressures studied so far for each. Transport and spectroscopic measurements up to megabar pressures are needed to fully characterize these cuprates and explore higher possible critical temperatures in these materials.

DOI: 10.1103/PhysRevMaterials.7.064803

I. INTRODUCTION

The nature of unconventional superconductivity in the cuprates is a subject of continued study [1,2]. Decades of evidence support the hypothesis that superconductivity in these compounds is a quasi-two-dimensional phenomenon that emerges from the layers of parallel CuO_2 planes common to these materials [3–6]. The critical temperature (T_c) in the materials can therefore be modified by altering the electronic structure of the CuO_2 planes. Though these changes in T_c are typically conducted by variable oxygen doping [7], the application of pressure can also tune T_c in the cuprates in an analogous manner [8–13]. The tendency for the T_c-P relation to follow a roughly parabolic trajectory that parallels the doping dependence of T_c is reported in nearly all known superconducting cuprates (see reviews [14–16] and references therein). Understanding the nature of unconventional superconductivity, along with the potential to carefully engineer strain conditions to further enhance T_c [17,18], necessitates high-pressure structural and equation of state (EOS) studies of these materials.

The effect of pressure on the bismuth-based cuprate superconductors [$Bi_2Sr_2Ca_{n-1}Cu_nO_{2n+4+\delta}$ ($n = 1$–3) (BSCCO)] is particularly intriguing. In all three compounds, T_c is observed first to increase, then decrease on further compression [19–22]. The behavior of T_c upon continued pressurization is dependent on both compression environment and oxygen doping; in some experiments, T_c as measured using high-pressure resistance and ac susceptibility techniques continues to decrease, and superconductivity is eventually destroyed [21], while in other experiments as pressure is increased T_c breaks away from the domelike trend and increases to the maximum pressures reported for each compound. Chen *et al.* [19] discovered this "up-down-up" trajectory with pressure in $Bi_2Sr_2Ca_2Cu_3O_{10+\delta}$ (Bi-2223) with the second increase beginning at 25 GPa. Deng *et al.* [20] later found this behavior in $Bi_2Sr_2CuO_{6+\delta}$ (Bi-2201) and in $Bi_2Sr_2CaCu_2O_{8+\delta}$ (Bi-2212), where the second rise in T_c begins at 45 and 40 GPa, respectively. Similarly, nonmonotonic T_c pressure dependencies have not been reported to date in any other cuprate superconductors. All compounds are reported to maintain a layered perovskite structure (Fig. 1) to at least 50 GPa [23–25], so these changes in T_c can be directly correlated with compression of the prototype structure of each. In contrast, other cuprate superconductors undergo pressure-induced structural transitions [26–29] including hysteresis effects [30,31] which can influence or destroy superconductivity.

High-pressure structural data have been reported for Bi-2212 [21,32–34], but the results are conflicting. Olsen *et al.* [32] studied compression of a mixed-phase sample of Bi-2212 and Bi-2223 to 50 GPa using energy-dispersive x-ray diffraction (XRD). The group observed a stiffening of the

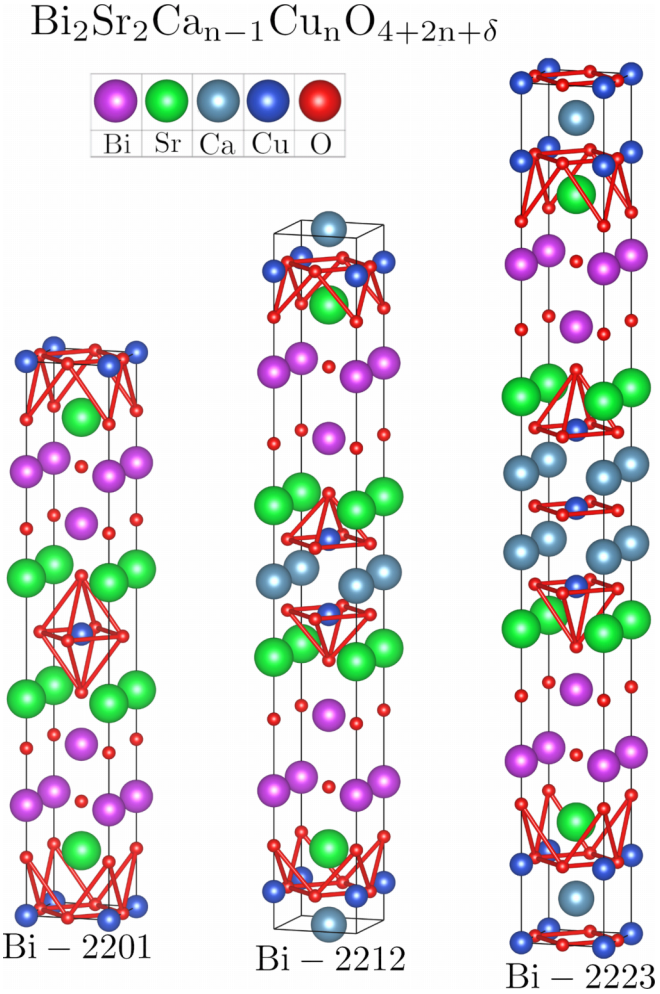

FIG. 1. Unit cells of Bi-2201, Bi-2212, and Bi-2223 presented in a tetragonal ($I4/mmm$) representation. Structural parameters for Bi-2201 from Matheis *et al.* [101] and for Bi-2212 and Bi-2223 from Wesche *et al.* [102].

c parameter near 20 GPa, followed by a drastic decrease in c between 35 and 40 GPa. Deng *et al.* [20] noted that this decrease occurs near the pressure of the rise in T_c in Bi-2212, and they suggested that this structural change arises from a pressure-induced Lifshitz transition. Zhang *et al.* [34] reported significantly different pressure-induced distortions in Bi-2212 on compression, specifically proposing a transition from the orthorhombic (pseudotetragonal) structure to a "collapsed orthorhombic" structure near 20 GPa. Zhang *et al.* [34] observed a pressure-induced stiffening in c near 20 GPa, but did not reach the pressures where the collapse in c had been reported [32]. In addition to these structural discrepancies, considerable differences in EOS parameters for the $n = 1, 2, 3$ varieties of BSCCO have been reported [32,34–40]. For example, EOS parameters obtained from fitting x-ray diffraction data for Bi-2212 result in a bulk modulus (K_0) of 60–130 GPa [21,32–34], whereas direct ambient pressure ultrasonic measurements typically give much lower K_0 values of 15–40 GPa [38,39,41].

Here we report a detailed structural and EOS study of $Bi_2Sr_2Ca_{n-1}Cu_nO_{2n+4+\delta}$ ($n = 1, 2, 3$) compounds (Bi-2201, Bi-2212, and Bi-2223, respectively) under quasihydrostatic compression up to megabar pressures. Quasihydrostatic conditions were achieved by pressurizing samples with a neon medium [42], which remains significantly more hydrostatic under pressure than the media used in the past for BSCCO [43]. This approach allows us to measure the compressive properties of BSCCO under considerably more hydrostatic stresses and extend the pressure range of reported P-V data. Experiments were also performed using no pressure-transmitting medium in order to compare with our quasihydrostatic and previous nonhydrostatic results. The data reveal all three BSCCO compounds to be highly susceptible to deviatoric stress. We now attribute many of the previously reported pressure-induced structural distortions to artifacts induced by nonhydrostatic stress conditions. Additionally, even when compressed quasihydrostatically, all three materials exhibit anomalous compression with P-V relations not well described by a single standard EOS formulation.

II. METHODS

Samples were loaded in symmetric diamond anvil cells (DACs) with diamond culet sizes ranging from 300 to 600 μm. The single-crystal Bi-2201 and Bi-2212 samples were optimally doped and synthesized at the Houston Center for Superconductivity. Sintered pellets of Bi-2212 + Bi-2223 were purchased from Quantum Levitation. Composition and ambient pressure unit-cell volumes (V_0) were determined using ambient pressure XRD utilizing a Bruker D8 Advance diffractometer with a Cu source. The volume ratio of the Bi-2223/Bi-2212 samples was estimated to be 80%/20%. All samples were ground into a fine powder using an agate mortar and pestle. Tungsten and rhenium gaskets were preindented to 20 GPa, and holes of 50–150 μm in diameter were laser-drilled to form the sample chambers [44]. Samples were loaded in DACs along with neon as a pressure-transmitting medium (for our quasihydrostatic runs) at GSECARS, Sector 13, APS, ANL [42]. Neon was chosen for these experiments because, even after pressure-induced freezing at 4.8 GPa at room temperature [45], the material remains a weak solid to megabar pressures [46] and is considerably more hydrostatic than the pressure-transmitting media used in past BSCCO x-ray diffraction studies [21,32–34,43]. X-ray diffraction was measured at the 16-IDB and 16-BMD beamlines at HPCAT, Sector 16, APS, ANL [47]. Pressures were determined from lattice parameters obtained by XRD of gold flakes placed within the sample chamber using the EOS of Anderson *et al.* [48]. The pressures were consistent with those determined by ruby fluorescence measurements using the Xu *et al.* [49] calibration. The sample detector distance was calibrated with a CeO_2 standard, and the x-ray diffraction patterns were integrated using the DIOPTAS software package [50].

The zero-pressure bulk modulus (K_0) and its pressure derivative ($K_0' = \frac{dK_0}{dP}$) were determined by fitting the P-V data to standard phenomenological EOS functions. The Vinet EOS [51] is written

$$P = 3K_0\left(\frac{1-\eta}{\eta^2}\right)\exp\left[\frac{3}{2}(K_0'-1)(1-\eta)\right], \qquad (1)$$

where $\eta = (V/V_0)^{\frac{1}{3}}$ is the strain, and it was found to be the most useful for analyses of the compression mechanisms of these materials. The EOS can be linearized in terms of η, and $H(\eta) = P\eta^2/3(1-\eta)$, and it is written as

$$\ln(H(\eta)) = \ln(K_0) + \tfrac{3}{2}(K_0' - 1)(1-\eta). \quad (2)$$

Deviations from linearity in the plot of $\ln(H(\eta))$ versus $1-\eta$ can be used to assess pressure-induced changes in the compression properties of the material, as we show below.

III. RESULTS

Representative diffraction patterns for Bi-2201 and Bi-2212 + Bi-2223 are presented in Fig. 2 (for additional data, see Fig. S1 in the supplemental material [52]). BSCCO compounds are reported to maintain orthorhombic symmetry similar to the ambient pressure *Ammm* structure [23,24] over the pressure ranges studied to date [21,32–34]. At ambient pressures, the structures can be described as pseudotetragonal (space group $I4/mmm$) with $a - b \leqslant 0.1$ Å [32,33]. This representation appears to be valid at high pressure, and is adopted in the Le Bail refinements performed in this work using JANA 2006 [53] to determine lattice parameters. Patterns were fit to a unit cell with $a \approx 3.8$ Å and a compound-dependent c axis length. To directly compare with past results, in which the ab plane of the primitive unit cell was rotated 45° in order to place the cell boundary along the Cu-Cu bond resulting in an ambient pressure $a \approx 5.4$ Å, the a parameters from our refinements were multiplied by $\sqrt{2}$. Though BSCCO compounds are known to exhibit both commensurate [54,55] and incommensurate [55–57] modulations along the b and c axes, diffraction peaks arising from these modulations are weak and were not observed, as in previous high-pressure experiments [58]. For the three materials, all prominent diffraction peaks in the collected diffraction patterns were indexed to standard Bragg reflections. We now discuss the results for each composition.

A. Bi-2201

The diffraction data for Bi-2201 can be described with ambient pressure pseudotetragonal unit-cell parameters $a = 5.31(1)$ Å and $c = 24.6(1)$ Å in good agreement with previous reports (see the supplemental material [52], Table S1, and Refs. [59–61] therein). Given the inhomogeneously broadened linewidths, weak orthorhombic distortions up to 0.05% cannot be ruled out. Several peaks in the diffraction patterns [Fig. 2(a)] are attributed to a small amount of Bi_2O_3, a common precursor material in BSCCO synthesis [60] still present in the sample; the pressure dependence of these peaks is consistent with previously reported data [62,63]. The a and c lattice parameters of Bi-2201 are found to decrease monotonically with pressure [Fig. 3(a)]; a decreases smoothly with pressure whereas c decreases but becomes less compressible between 8 and 10 GPa. This change in compressibility is clearly evident in the pressure dependence of the c/a ratio [Fig. 3(b)].

Fitting the entire dataset to a single Vinet EOS with a fixed V_0 determined using ambient pressure x-ray data resulted

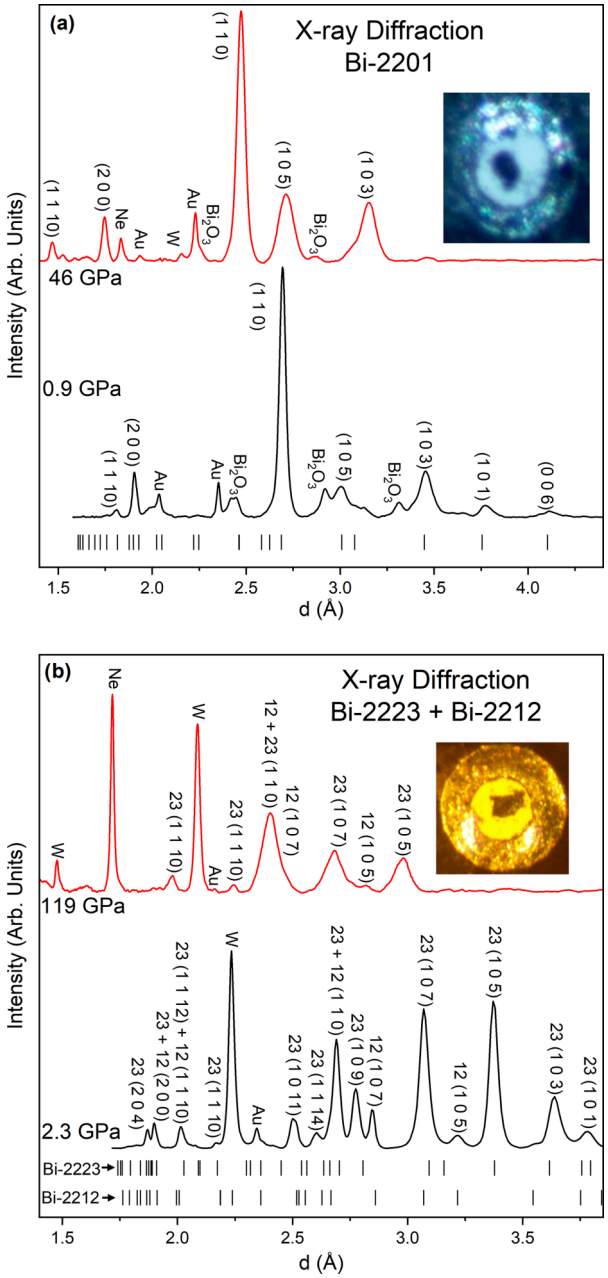

FIG. 2. Representative integrated x-ray diffraction patterns for BSCCO samples. All patterns were fit to a tetragonal $I4/mmm$ symmetry unit cell with ambient pressure parameters given in the text. (a) Diffraction patterns for Bi-2201 taken at 0.9 GPa (black) and 46 GPa (red) ($\lambda = 0.4959$ Å). Tick marks indicate predicted Bragg peaks for Bi-2201 at 0.9 GPa. Peaks from unreacted Bi_2O_3 from synthesis are identified in the pattern. The inset is a reflected light micrograph of the sample loaded in the DAC at 0.9 GPa with a 150 μm sample chamber diameter surrounded by the Ne pressure-transmitting medium. (b) Diffraction patterns of mixed-phase Bi-2212 + Bi-2223 at 2.3 GPa (black, $\lambda = 0.406\,626$ Å) and 119 GPa (red, $\lambda = 0.4133$ Å). Both are indexed using tetragonal $I4/mmm$ symmetry. Tick marks indicate predicted Bragg peaks of Bi-2223 (black) and Bi-2212 (red) at 2.3 GPa. Diffraction from the pressure-transmitting medium Ne (above freezing pressure) and W from the gasket are identified. The inset is a reflected light micrograph of mixed-phase Bi-2212 and Bi-2223 at 2.3 GPa in the DAC with a 150 μm sample chamber surrounded by the Ne medium.

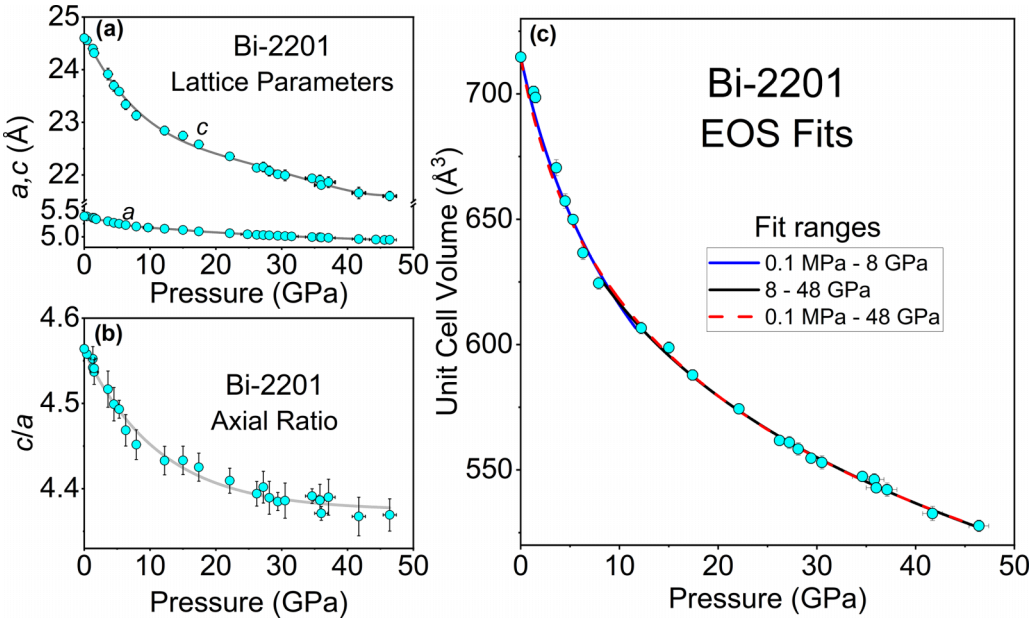

FIG. 3. Pressure dependence of the structural parameters of Bi-2201. (a) a (red) and c (blue) parameters of Bi-2201. (b) c/a ratio of Bi-2212, showing a change in the observed trend between 8 and 10 GPa. Lines inserted as guides to the eye. (c) Unit-cell volume with Vinet EOS fit to the data over three pressure ranges, 0.1 MPa–48 GPa [$V_0 = 714.7$ Å^3, $K_0 = 32.0(1.3)$ GPa, $K_0' = 10.7(3)$], 0.1 MPa–8 GPa [$V_0 = 714.7$ Å^3, $K_0 = 54.6(1.3)$ GPa, $K_0' = 0.57(3)$], and 8–48 GPa [$V_0 = 696.6(4.0)$ Å^3, $K_0 = 45.8(3.4)$ GPa, $K_0' = 9.6(4)$]. For pressure ranges including zero pressure, the fixed value of $V_0 = 714.7$ Å^3 is that determined from ambient pressure x-ray diffraction. All error bars represent 1σ uncertainty.

in unacceptably large residuals, whereas above 10 GPa the residuals are much smaller. We are able to greatly improve the fits by splitting the data into two regions, above and below the point of stiffening in c at 8 GPa [Fig. 3(c)]. In the high-pressure fit, all three parameters were allowed to vary, while the low-pressure fits V_0 were fixed to 714.67 Å^3, which we measured at ambient pressure. Fitting parameters from this work and previously measured values of K_0 are presented in Table I and discussed below.

B. Bi-2212

X-ray diffraction of single-phase Bi-2212 and mixed-phase Bi-2212 + Bi-2223 was measured up to 61 and 155 GPa, respectively, over five experimental runs. In the diffraction patterns of the mixed-phase samples, structural data from the minority phase Bi-2212 were extracted up to 108 GPa before low intensities, and broad peaks prevented acceptable refinements. Similar to Bi-2201, the patterns for all samples can be described with pseudotetragonal $I4/mmm$ symmetry with $a \approx b$ similar to previous reports (see Table S2 in the supplemental material [52] and Refs. [23,33,53,58,64–69] therein). Both a and c decrease monotonically, and c exhibits a stiffening at 18–20 GPa [Figs. 4(a) and 4(b)].

TABLE I. K_0 and K_0' values from this work and reported in the literature for Bi-2201 using x-ray diffraction (XRD) and ultrasonic methods; uncertainties are included when provided. Our data are not well described by a single EOS. The K_0 values reported for the ultrasonic data are systematically lower. Data from Dominec *et al.* [35]

K_0 (GPa)	K_0'	Technique	Source
54.6(1.3)	0.57(3)	XRD (0.1 MPa–8 GPa)	This work
45.8(3.4)	9.6(4)	XRD (8–48 GPa)	This work
15.3	–	Ultrasonic	Dominec *et al.* [35]
18.9	–	Ultrasonic	Dominec *et al.* [35]

Below 10 GPa our P-V data are in excellent agreement with previously reported results, including the reported onset of stiffening in c [32,34]. At higher pressures, however, our quasihydrostatic data diverge from previous reports. Whereas Olsen *et al.* [32] observed a decrease of nearly 7% in the c/a axial ratio from 38 to 42 GPa, our data indicate that the axial ratio saturates at pressures above 20 GPa and remains roughly constant to the upper pressure limit of our measurement. We find no evidence for the reported collapsed orthorhombic phase under pressure [34]. A pseudotetragonal unit cell well describes the structure over the pressure range of our experiments: The pressure dependence of a and b remains close over the measured range, and no anomalous increase in a or b is observed. In addition, above 15 GPa our unit-cell volumes are consistently lower than those reported previously [21] (Fig. 4).

To test the impact of nonhydrostaticity on the compression of Bi-2212, we measured x-ray diffraction on samples without a transmitting medium by directly compressing a sample of mixed-phase Bi-2212 + Bi-2223 between two diamonds. This nonhydrostatic compression exhibited several anomalies in the a and c parameters similar to those observed in previous experiments. Most notably, we observe a pressure-induced increase in a similar to that observed by Zhang *et al.* [34], and a series of collapses in c similar to those observed by Olsen *et al.* [32]. A quantitative comparison between the

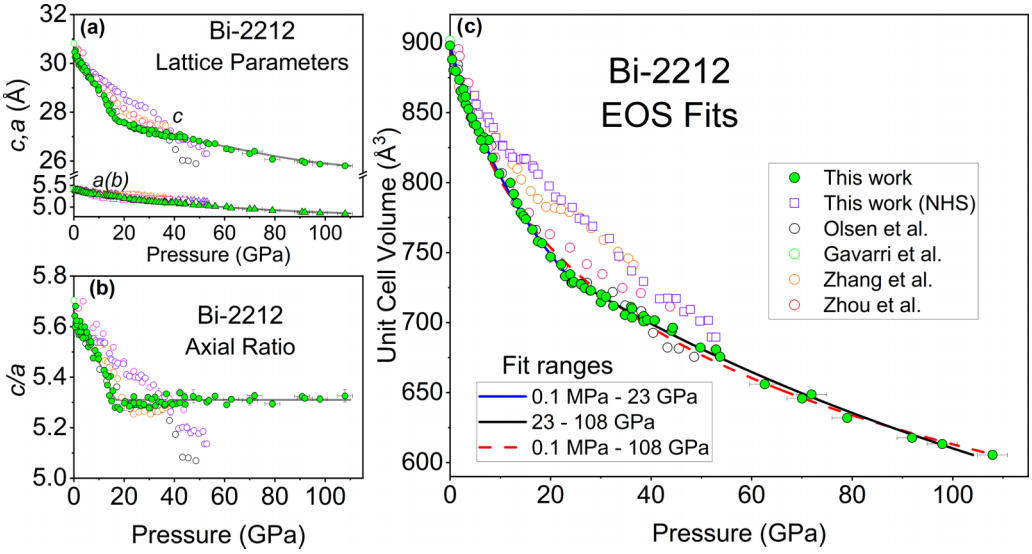

FIG. 4. Pressure dependence of the structural parameters of Bi-2212 measured under quasihydrostatic conditions (this work, green solid circles) and nonhydrostatic conditions (NHS; this work, open purple squares) and previous results, Olsen *et al.* [32], Gavarri *et al.* [33], Zhang *et al.* [34], and Zhou *et al.* [21]. (a) a (triangles), b (inverted triangles), and c (circles) lattice parameters. Lines inserted as guides to the eye. (b) c/a axial ratio, showing a change in compression mechanism at 23 GPa, coinciding with the stiffening of c. (c) Pressure dependence of the unit-cell volume and Vinet EOS fit to the data over three pressure ranges, 0.1 MPa–108 GPa [$V_0 = 898.0$ Å^3, $K_0 = 53.9(1.6)$ GPa, $K_0' = 8.7(2)$] 0.1 MPa–23 GPa [$V_0 = 898.0$ Å^3, $K_0 = 67.7(2.3)$ GPa, $K_0' = 4.9(3)$], and 23–108 GPa [$V_0 = 793.9(4.6)$ Å^3, $K_0 = 262.8(22.4)$ GPa, $K_0' = 2.9(4)$]. For pressure ranges containing ambient pressure (0.1 MPa), V_0 was fixed to 898.0 Å^3, a value obtained by ambient pressure XRD. Low-pressure and high-pressure fits produce K_0 and K_0' values in agreement with each other over similar pressure ranges. For all plots, error bars represent 1σ uncertainty.

features apparent in our nonhydrostatic experiment and those present in previously reported data is not possible because the degree of nonhydrostaticity depends on unreported details of the previous experiments.

When fitting all quasihydrostatic data (0.1 MPa–108 GPa) to a single EOS, we obtain K_0 and K_0' values in disagreement with those reported in the literature for data based on analysis of high-pressure x-ray diffraction data [21,32,34,36,37]. These discrepancies motivated us to fit the data over multiple different pressure regimes as was done for Bi-2201. A cutoff of 22 GPa was chosen due to the stiffening in the c parameter apparent in Bi-2212 beginning at this pressure [Fig. 4(b)]. For ranges that contain ambient pressure, a fixed $V_0 = 898.4$ Å^3 was used, as determined from ambient pressure x-ray diffraction, with K_0 and K_0' allowed to vary. Above 22 GPa, the data were fit to a Vinet EOS with all parameters allowed to vary. Splitting P-V data in this way greatly improves the fits over the entire pressure range, and results in low-pressure K_0 and K_0' values that agree with previous compression experiments [21,32,34,36,37]. As discussed below, the K_0 and K_0' determined from fitting high-pressure data can differ significantly from those measured using ultrasonic techniques at ambient pressure (Table II) [38,39].

C. Bi-2223

XRD from the mixed-phase Bi-2212 + Bi-2223 samples provided structural information of Bi-2223 to 155 GPa. Similar to the other two materials, the XRD patterns are well described by a pseudotetragonal $I4/mmm$ structure with ambient pressure lattice parameters [$a = 5.396(5)$ Å, $c = 30.070(5)$ Å] in agreement with previously reported results (see the supplemental material [52], Table 3, and Refs. [70–72] therein). Pressure dependencies of the structural parameters of Bi-2223 are presented in Fig. 5. Like Bi-2201 and Bi-2212, no change in the compression of the a axis was apparent, and a slight kink in c was observed at 30 GPa, which is more obvious in the pressure dependence of the c/a ratio [Fig. 5(b)]. As with Bi-2201 and Bi-2212, this feature appears to be due to a stiffening in the c axis.

TABLE II. K_0 and K_0' values from this work and reported previously for Bi-2212; uncertainties included when provided. Data from Olsen *et al.* [32], Tajima *et al.* [36], Zhang *et al.* [34], Yoneda *et al.* [37], Solunke *et al.* [38], Fanggao *et al.* [39], Munro *et al.* [40], and Dominec *et al.* [35].

K_0 (GPa)	K_0'	Technique	Source
70.5(1.8)	4.9(3)	XRD (0.1 MPa–23 GPa)	This work
262.8(22.4)	2.9(4)	XRD (23–108 GPa)	This work
62(5)	6.0(3)	XRD	Olsen *et al.* [32]
73	–	XRD	Tajima *et al.* [36]
127(11)	4(fixed)	XRD	Zhang *et al.* [34]
61	–	XRD (Pb-doped)	Yoneda *et al.* [37]
26.34	–	Ultrasonic	Solunke *et al.* [38]
20.18	–	Ultrasonic	Solunke *et al.* [38]
26.4	40	Ultrasonic (Pb-doped)	Fanggao *et al.* [39]
15.4	–	Ultrasonic	Fanggao *et al.* [39]
21.9	–	Ultrasonic	Munro *et al.* [40]
10.9	–	Ultrasonic	Dominec *et al.* [35]

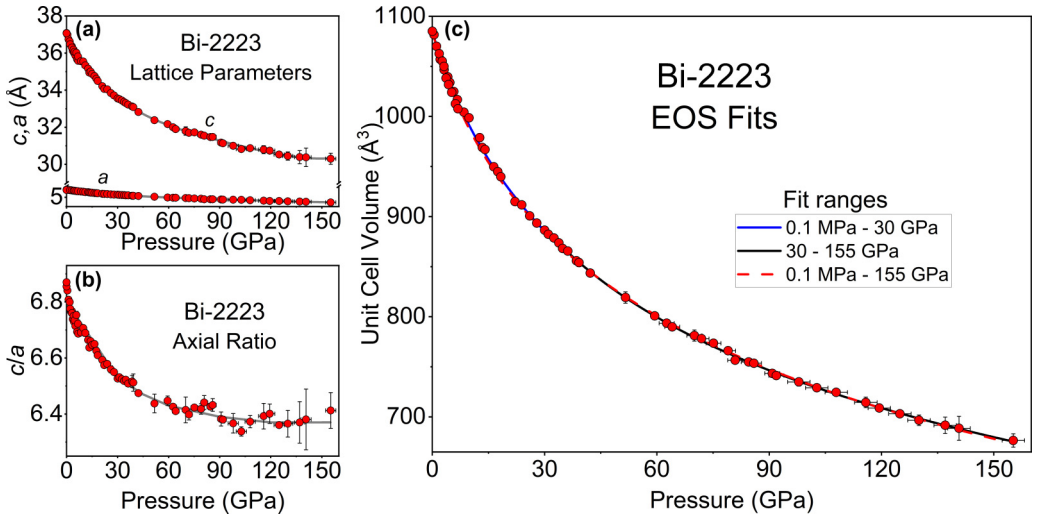

FIG. 5. Pressure dependence of the structural parameters of Bi-2223. (a) a and c parameters. Lines inserted as guides to the eye. (b) c/a ratio for Bi-2223. (c) Unit-cell volume with Vinet EOS fit to the data over three pressure ranges, 0.1 MPa–155 GPa [$V_0 = 1085.0$ Å^3, $K_0 = 77.7(9)$ GPa, $K_0' = 6.4(1)$], 0.1 MPa–30 GPa [$V_0 = 1085.0$ Å^3, $K_0 = 84.9(2)$ GPa, $K_0' = 5.6(4)$], and 30–155 GPa [$V_0 = 1179(36)$ Å^3, $K_0 = 35.5(9)$ GPa, $K_0' = 7.9(5)$]. For pressure ranges including ambient pressure (0.1 MPa), V_0 was fixed to 1085.0 Å^3, a value obtained from ambient pressure x-ray diffraction. All error bars represent 1σ uncertainty.

Similar to the other two compounds, the data could not be fit to a single EOS over the entire pressure range studied. Attempting to fit the data to a single EOS resulted in unacceptably large residuals, especially below 30 GPa [Fig. 5(c)]. Therefore, the data were split into two regimes at 30 GPa and fit to two separate EOS. Similar to Bi-2201 and Bi-2212, splitting the fits resulted in V_0, K_0, and K_0' parameters with significantly smaller residuals and uncertainties [Fig. 5(c)]. Fits that constrained the volume at ambient pressure used a fixed $V_0 = 1085.0$ Å^3, which we determined using ambient pressure XRD. As observed in Bi-2201 and Bi-2212, the fitting parameters obtained for Bi-2223 disagree with the ambient pressure values of K_0 and K_0' reported previously (Table III).

TABLE III. K_0 and K_0' values from this work and reported in the literature for Bi-2223; uncertainties are included when provided. There is a probe-dependent discrepancy in K_0 and K_0' values and our data are not well described by a single EOS (See text). The change in compression mechanism revealed through the stress-strain relation demonstrates the need to fit the data to a high- and low-pressure EOS. Multiple values from the same source indicate different sample runs. Data from Yoneda *et al.* [37], Fanggao *et al.* [39], and Dominec *et al.* [35].

K_0 (GPa)	K_0'	Technique	Source
100.9(2.3)	4.1(3)	XRD (0.1 MPa–30 GPa)	This work
34.3(1.6)	8.1(5)	XRD (30–155 GPa)	This work
73	–	XRD	Yoneda *et al.* [37]
18.9	59	Ultrasonic (Pb doped)	Fanggao *et al.* [39]
22.9	39.3	Ultrasonic (Pb doped)	Fanggao *et al.* [39]
26.5	–	Ultrasonic	Dominec *et al.* [35]
22.0	–	Ultrasonic	Dominec *et al.* [35]
15.5	–	Ultrasonic	Dominec *et al.* [35]
22.1	–	Ultrasonic	Dominec *et al.* [35]

IV. DISCUSSION

A. Equation-of-state fits

Detailed fitting of the P-V data for all three materials to a single phenomenological EOS over the entire measured pressure range produces large residuals, especially at low pressures. This result is independent of which condensed phase EOS function is used (e.g., Vinet versus Birch-Murnaghan [73]). Only the fits using the Vinet EOS are presented here. Fitting P-V data in different regimes produces much improved fits. In the lower-pressure range, EOS fitted parameters are expected to match those obtained from other methods, such as the ultrasonic determination of the ambient pressure bulk modulus for a sample of the same density, suitably corrected from adiabatic to isothermal conditions [74]. If all the data are used, our fitted EOS parameters and those previously reported based on high-pressure x-ray diffraction [34,36,37,68] disagree with those using ultrasonic techniques [35,38–40]. We note that some disagreement in the measured K_0 may be attributed to porosity and lattice defects in as-grown cuprate superconductors [75,76], which are known to be particularly prevalent in Bi-2201 [77,78] and Bi-2223 samples [70]. These defects most likely account for the large spread in measured adiabatic K_0 values reported for Bi-2212 (Table II) and Bi-2223 (Table III). Differences in the degree of strain throughout the samples will result in the measured K_0 falling between the Voigt [79] and Reuss [80] bounds, but the bounds are two to three times smaller than the range of K_0 values previously reported.

In Bi-2201, the low-pressure (below 8 GPa) fit produced a K_0 of 54.6(1.3) GPa, a value significantly larger than those determined using ultrasonic techniques [35,41], where $K_0 \approx$ 15–19 GPa (Table I). The fit above 8 GPa results in a K_0 of 45.8(3.4), which is still significantly larger than ambient pressure measurements. The discrepancy in these values further suggests anomalous compression of Bi-2201. The

low-pressure fit produced a K_0' of 0.57, significantly lower than most materials which are well described with a phenomenological EOS with $2 \leqslant K_0' \leqslant 8$ where most materials exhibit $K_0' \approx 4$ [81]. The Bi-2212 *P-V* data were fit to two separate compression regions with a pressure cutoff determined by the stiffening in c near 23 GPa, similar to the process used for Bi-2201. [Fig. 4(b)]. For the low-pressure fit, we find $K_0 \approx 70.5$ GPa, which is comparable to values measured previously using similar diffraction techniques [32,36,37]. The K_0 of Bi-2212 measured using ultrasonic techniques at ambient pressures, however, tend to be significantly lower than those determined via fitting an EOS to *P-V* data, with ultrasonic measurements yielding K_0 of 10–27 GPa [35,38–40]. The EOS fit to the low-pressure Bi-2212 data gives a $K_0' = 4.9(3)$, comparable to values obtained in previous compression studies over similar pressure ranges [35,38–40]. In contrast to compression experiments, analyses of ultrasonic measurements give K_0' as high as 40 [39]. We conclude there is a change in compression mechanism at 23 GPa for Bi-2212 irrespective of the pressure-transmitting medium used, with all compression data exhibiting some kink in the pressure dependence of c/a near this pressure.

For the high-pressure fit, K_0 drastically increases to 263(22) GPa, with K_0' decreasing from 4.9(3) to 2.9(4). This change is associated with a pressure-induced stiffening along the c axis similar to that reported for other perovskite-based structures such as $CaZrO_3$ [82] and the stiffening in b in $CaIrO_3$ [83]. This behavior correlates with the reported decrease in $\frac{dT_c}{dP}$ in Bi-2212 [20] [Fig. S4(b) [52]] and is consistent with pressure-induced charge-transfer models developed to describe the effect of pressure on T_c in the cuprates [8,84,85]. The correlation between the c axis and the change in T_c of Bi-2212 is consistent with recent STM measurements [86] in which the distance of the apical oxygen site to the CuO_2 layers (determined by c) impacts the superconducting pairing mechanism. No structural changes appear at pressures of the second T_c increase in any of the materials. Pressure-induced suppression of a competing electronic order [19] and a Lifshitz transition [20] have been proposed to explain the phenomenon; more detailed high-pressure studies are needed to investigate these possibilities.

Similar to the other Bi-based cuprates, fitting all Bi-2223 *P-V* data to a single Vinet EOS (0–155 GPa) results in poor fits. Splitting the fit into two pressure regions based on the kink in the pressure dependence of the c/a ratio at 30 GPa results in a much better fit with greatly reduced residuals. The low-pressure fit produces a $K_0 = 84(2)$ GPa and a $K_0' = 5.6(3)$. The K_0 from the fits are significantly larger than those reported from ultrasonic measurements, which give K_0 values of 15–40 GPa [35,39,41]. As with Bi-2212, K_0' is reported to be significantly larger when measured using ultrasonic probes, with Fanggao *et al.* [39] reporting values between 39 and 59 whereas our XRD measurements indicate $K_0' = 5.6(3)$. Our high-pressure fit produces a K_0 value of 35.5(8) GPa with $K_0' = 7.9(5)$. We attribute the discrepancies between our observed compression trends and the trends observed in the past primarily to the significant impact of deviatoric stress present in all samples, and to the intrinsic anomalous compression of the materials.

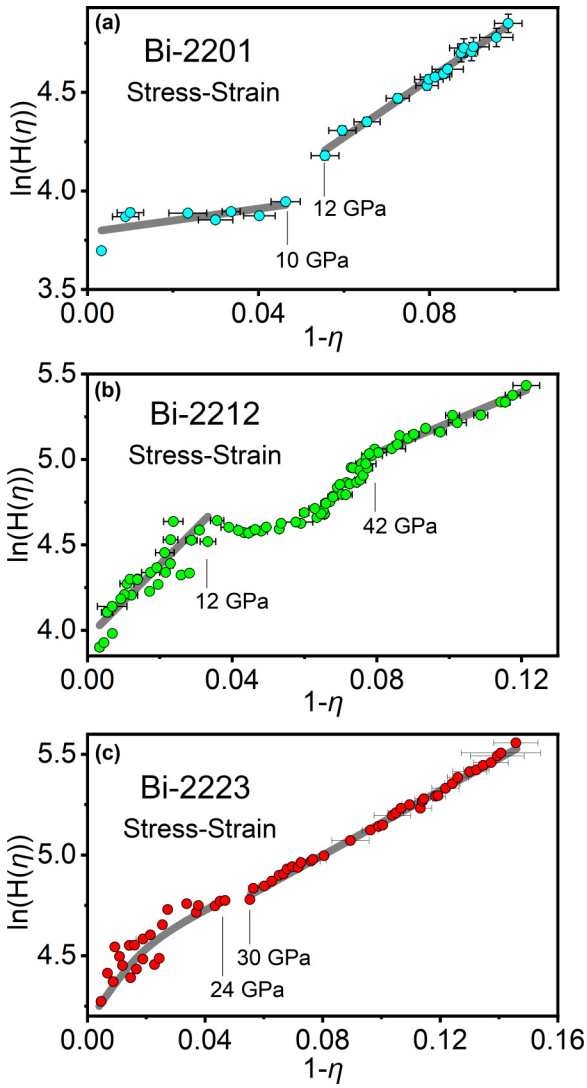

FIG. 6. Stress-strain relationships for the three compounds showing changes in compression mechanisms. The pressures corresponding to particular strains are indicated for each. (a) Bi-2201. (b) Bi-2212. (c) Bi-2223. Lines inserted as guides to the eye.

B. Stress-strain relations

Linearized stress-strain analyses were performed for each compound to further analyze the anomalies observed in the compression of these materials. Major changes in the trend of the stress-strain relation are present in all three materials demonstrating pressure-induced stiffening and anomalous compression mechanisms that are not well described by any of the common phenomenological EOS. The linearized compression data are presented in Fig. 6.

The stress-strain relationship for Bi-2201 is linear up to $(1 - \eta) \approx 0.5$, corresponding to 10 GPa, where a discontinuity is apparent. This feature corresponds to the pressure of the "knee" feature in the pressure dependence of the c/a ratio, further reinforcing our use of multiple pressure cutoffs for fitting an EOS above and below 10 GPa. Above the discontinuity, the value of $\ln(H(\eta))$ increases linearly along with the slope of the stress-strain relation [Fig. 6(a)]. The same procedure applied

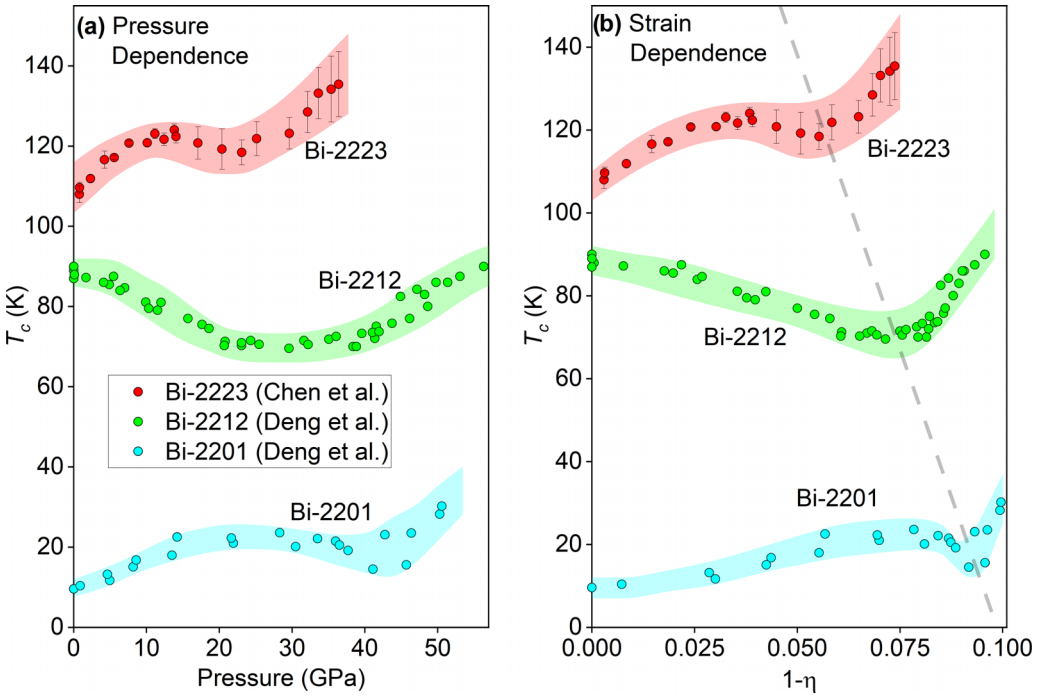

FIG. 7. (a) Previously measured pressure dependence of T_c for BSCCO compounds as reported by Chen *et al.* [19,103] and Deng *et al.* [20]. (b) Strain $(1-\eta)$ dependence of previously reported T_c values using the EOS measured in this work to convert pressure to strain. Dashed line inserted as a guide to the eye indicating strain where a second rise in T_c occurs.

to Bi-2212 [Fig. 6(b)] results in a deviation from linearity at $(1-\eta) \approx 0.4$. Between $(1-\eta) \approx 0.4$ and 0.8 (12–42 GPa), the relation is distinctly nonlinear, indicating a major change in compression mechanism. Linearity resumes, albeit with a smaller slope, above $(1-\eta) \approx 0.8$. The midpoint of this region of nonlinearity corresponds to ∼22 GPa, the pressure of the "knee" feature apparent in the pressure response of the c/a ratio. The large nonlinear region indicates a degree of anomalous compression that is not accounted for in a single phenomenological EOS, with K_0 changing rapidly with pressure. Similar to Bi-2201, this result demonstrates that the compression of Bi-2212 is not well described by a single Vinet EOS over all pressure ranges. For a comparison between quasihydrostatic and nonhydrostatic stress-strain relations in Bi-2212; see Fig. S2 [52]. Finally, the linearized compression data for Bi-2223 [Fig. 6(c)] reveal a kink at $1-\eta = 0.05$ corresponding to a pressure of 30 GPa. Similar to the other two materials, this kink is in agreement with the kink in the pressure dependence of c/a. This indicates a change in the compression mechanism similar to that observed in Bi-2201 and Bi-2212, but much less pronounced. Quasihydrostatic and nonhydrostatic stress-strain relations for Bi 2223 are presented in the supplemental material [52], Fig. S3. All stress-strain relations reveal distinct high- and low-pressure compression regions in the three compounds.

The previously reported pressure dependence of T_c [19,20] [Fig. 7(a)] is converted into a strain dependence using our stress-strain relation. The $1-\eta$ dependence of T_c is presented in Fig. 7(b). The strain dependence demonstrates that the large decrease in the magnitude of the observed $\frac{dT_c}{dP}$ in Bi-2212 is not apparent when removing the influence of changing compression mechanisms (i.e., the stiffening in c) from the T_c relation. The observation that the flattening of $\frac{dT_c}{dP}$ is not apparent when converting the data to $\frac{dT_c}{d(1-\eta)}$ and removing any influence from stiffening in c corroborates the commonly used pressure-induced charge-transfer model [8,84,85] in which the proximity of the CuO_2 planes to the rocksalt-like charge reservoir layers is responsible for the initial "up-down" pressure dependence of T_c in these cuprates. Converting the data to show the strain dependence more clearly suggests that the second rise in T_c is related to the number of CuO_2 planes per unit cell, with more planes associated with a second increase in T_c at lower strains and at a lower rate with respect to $1-\eta$.

C. Anomalous compression

Even when fitting an EOS to the P-V data below the obvious discontinuities in the stress-strain relations, the K_0 values that emerge from the fits are significantly larger than those obtained ultrasonically. If these fitting parameters were representative of the true K_0 and K_0', one would expect similar values to be measured irrespective of the technique used. The analysis reveals an anomalous compression mechanism even at low pressures. This discrepancy is exemplified in our P-V data for all three BSCCO compounds, where fitting the data at pressures below the discontinuities in the stress-strain relationships results in K_0 values significantly larger than those measured in ultrasonic experiments [35,38–40]. Reducing the upper pressure cutoff used in the fits results in the resultant K_0 value decreasing and eventually converging with the ambient pressure values. In contrast to the behavior of BSCCO, performing a similar analysis on P-V data in the literature for the simple materials MgO [87], CaO [88], LiF [89], and NaCl [89,90] results in similar values of K_0 that are consistent

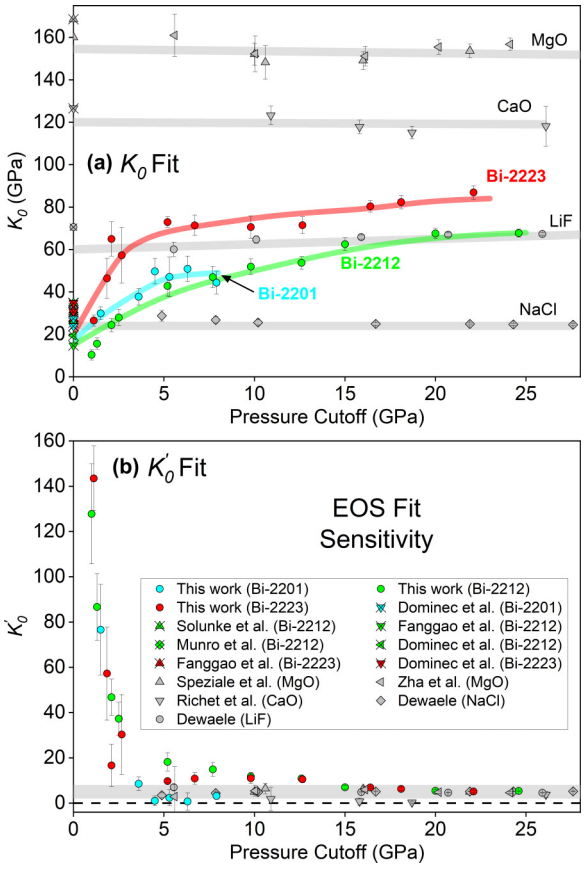

FIG. 8. Sensitivity of Vinet EOS fit parameters for BSCCO compared to selected simple compounds. (a) Sensitivity of K_0 to pressure cutoff for BSCCO and for MgO, CaO, LiF, and NaCl. Data points with an X indicate values measured at ambient pressures using ultrasonic techniques. For simple compounds, the fit values of K_0 are relatively independent of cutoff pressure and agree with the ultrasonic zero-pressure values, whereas for BSCCO the fit values of K_0 disagree with those measured at zero pressure when a large cutoff is used in the fitting process. Reducing the upper pressure cutoff used in the fit causes the resultant K_0 to approach the zero-pressure values. (b) Sensitivity of K_0' to upper pressure cutoff, demonstrating that the fit K_0' for simple materials is cutoff-independent and typically between 2 and 8 (shaded region), whereas for BSCCO, K_0' rapidly increases up to approximately 150 as the cutoff is decreased. For all samples, the increase in uncertainties as the cutoff pressure is lowered is due to fewer data points being used in the fits. Data from Speziale *et al.* [87], Richet *et al.* [88], Dewaele [89], Fanggao *et al.* [39], Seetawan [41], Dominec *et al.* [35], Solunke *et al.* [38], Munro *et al.* [40], and Zha *et al.* [104].

with the measured ambient pressure values irrespective of the upper pressure cutoff. The EOS relations of most conventional materials have values of K_0' of 2–8 [81,91–93]. The fit K_0' values of the aforementioned analysis on MgO [87], CaO [88], LiF [89], and NaCl [89,90] are nearly independent of the upper pressure cutoff used. All varieties of BSCCO, however, produce fitted values of K_0' that are highly dependent on the pressure range measured. Reducing the upper pressure cutoff for the BSCCO P-V data results in significantly larger K_0' values for cutoffs below ∼5 GPa. The cutoff pressure dependence on the fit values of K_0 and K_0' for BSCCO and selected simple materials are contrasted in Fig. 8.

V. CONCLUSIONS

We report structural and equation-of-state measurements for $Bi_2Sr_2Ca_{n-1}Cu_nO_{2n+4+\delta}$ ($n = 1, 2, 3$) under quasihydrostatic compression well beyond the pressure range of previous work. These results clarify and resolve discrepancies reported in the literature, and they provide information on the structural influence on the electronic structure and critical temperature of these materials. This work indicates that all three BSCCO compounds are highly susceptible to deviatoric stress, and that a structural modification does not coincide with the rise in T_c present in all three compounds under quasihydrostatic compression. It remains to be seen if other cuprates are as susceptible to deviatoric stress as the Bi-based compounds. Available data suggest that the presence of large deviatoric stresses in high-pressure experiments can suppress the maximum value of T_c [67,94–100]. Additionally, we conclude that the discrepancies in the reported K_0 and K_0' for all three materials arise from unusual compression mechanisms beginning at very low pressures (<10 GPa) that are not well described by conventional equations of state. We propose that the anomalous high-pressure behavior present in all BSCCO compounds is a manifestation of the changes in electronic properties that also give rise to the remarkable nonmonotonic dependence of T_c with pressure. These results cast high-pressure studies of BSCCO compounds, and of cuprate high-temperature superconductors in general, in a new light. The extent to which this anomalous compression and its relationship changes in T_c in other cuprate high-temperature superconductors remains to be explored.

ACKNOWLEDGMENTS

We are grateful to S. A. Gramsch, F. Restrepo, H. Aoki, and L. Sun for comments on the paper and/or helpful discussions; C. Li, H. Farraj, K. Kumar, and J. Cabana for assisting with the ambient pressure x-ray diffraction; S. Tkachev and R. Ferry for help in sample gas loading; and K. Lynch, D. Kuntzelman, R. Dojutrek, R. Frueh, J. Dublin, and M. Litz of the University of Illinois Chicago machine shop for fabricating the high-pressure cells. This work was supported by the US NSF (DMR-2104881) and DOE-NNSA (DE-NA0003975, CDAC), US Air Force Office of Scientific Research Grants FA9550-15-1-236 and FA9550-20-1-0068, the T.L.L. Temple Foundation, the John J. and Rebecca Moores Endowment, and the State of Texas through the Texas Center for Superconductivity at the University of Houston (TCSUH).

[1] C. W. Chu, L. Z. Deng, and B. Lv, Hole-doped cuprate high temperature superconductors, Physica C **514**, 290 (2015).

[2] D. F. Agterberg, J. S. Davis, S. D. Edkins, E. Fradkin, D. J. Van Harlingen, S. A. Kivelson, P. A. Lee, L. Radzihovsky, J. M.

Tranquada, and Y. Wang, The physics of pair-density waves: cuprate superconductors and beyond, Annu. Rev. Condens. Matter Phys. **11**, 231 (2020).

[3] W. E. Pickett, Electronic structure of the high-temperature oxide superconductors, Rev. Mod. Phys. **61**, 433 (1989).

[4] A. Damascelli, Z. Hussain, and Z.-X. Shen, Angle-resolved photoemission studies of the cuprate superconductors, Rev. Mod. Phys. **75**, 473 (2003).

[5] G. Logvenov, A. Gozar, and I. Bozovic, High-Temperature Superconductivity in a Single Copper-Oxygen Plane, Science **326**, 699 (2009).

[6] A. T. Bollinger and I. Božović, Two-dimensional superconductivity in the cuprates revealed by atomic-layer-by-layer molecular beam epitaxy, Supercond. Sci. Technol. **29**, 103001 (2016).

[7] A. Kaminski, S. Rosenkranz, H. M. Fretwell, M. R. Norman, M. Randeria, J. C. Campuzano, J.-M. Park, Z. Z. Li, and H. Raffy, Change of Fermi-surface topology in $Bi_2Sr_2CaCu_2O_{8+\delta}$ with doping, Phys. Rev. B **73**, 174511 (2006).

[8] M. Osada, M. Kakihana, T. Asai, H. Arashi, M. Käll, and L. Börjesson, High-pressure Raman study of $Bi_2Sr_2CaCu_2O_{8+\delta}$: indications of strong bond-strength hierarchy and pressure-induced charge transfer, Physica C **341–348**, 2241 (2000).

[9] M. Osada, M. Kakihana, M. Käll, and L. Börjesson, Pressure-induced effects in high-T_c superconductors: Raman scattering as a probe of charge-lattice dynamics under high pressure, Physica C **357–360**142 (2001).

[10] J. J. Neumeier and H. A. Zimmermann, Pressure dependence of the superconducting transition temperature of $YBa_2Cu_3O_7$ as a function of carrier concentration: A test for a simple charge-transfer model, Phys. Rev. B **47**, 8385 (1993).

[11] C. C. Almasan, S. H. Han, B. W. Lee, L. M. Paulius, M. B. Maple, B. W. Veal, J. W. Downey, A. P. Paulikas, Z. Fisk, and J. E. Schirber, Pressure Dependence of T_c and Charge Transfer in $YBa_2Cu_3O_x(6.35 < x < 7)$ Single Crystals, Phys. Rev. Lett. **69**, 680 (1992).

[12] C. Ambrosch-Draxl, E. Y. Sherman, H. Auer, and T. Thonhauser, Pressure-Induced Hole Doping of the Hg-Based Cuprate Superconductors, Phys. Rev. Lett. **92**, 187004 (2004).

[13] H. Sakakibara, K. Suzuki, H. Usui, K. Kuroki, R. Arita, D. J. Scalapino, and H. Aoki, Multiorbital analysis of the effects of uniaxial and hydrostatic pressure on T_c in the single-layered cuprate superconductors, Phys. Rev. B **86**, 134520 (2012).

[14] R. J. Wijngaarden, J. J. Scholtz, E. N. v. Eenige, K. Heeck, and R. Griessen, Pressure dependence of high-T_c superconductors, High Press. Res. **10**, 479 (1992).

[15] R. J. Wijngaarden, E. N. Van Eenige, J. J. Scholtz, D. T. Jover, R. Griessen, R. Winter, and J. Jonas, Ultra high pressure experiments on high-T_c superconductors, in *High Pressure Chemistry, Biochemistry and Materials Science*, edited by R. Winter and J. Jonas (Springer, Dordrecht, 1993), pp. 121–146.

[16] A. C. Mark, J. C. Campuzano, and R. J. Hemley, Progress and prospects for cuprate high temperature superconductors under pressure, High Press. Res. **42**, 137 (2022).

[17] E.-M. Choi, A. Di Bernardo, B. Zhu, P. Lu, H. Alpern, K. H. L. Zhang, T. Shapira, J. Feighan, X. Sun, J. Robinson, Y. Paltiel, O. Millo, H. Wang, Q. Jia, and J. L. MacManus-Driscoll, 3D strain-induced superconductivity in $La_2CuO_{4+\delta}$ using a simple vertically aligned nanocomposite approach, Sci. Adv. **5**eaav5532 (2019).

[18] J. Zhang, H. Wu, G. Zhao, L. Han, and J. Zhang, A review on strain study of cuprate superconductors, Nanomaterials **12**, 3340 (2022).

[19] X.-J. Chen, V. V. Struzhkin, Y. Yu, A. F. Goncharov, C.-T. Lin, H.-k. Mao, and R. J. Hemley, Enhancement of superconductivity by pressure-driven competition in electronic order, Nature **466**, 950 (2010).

[20] L. Deng, Y. Zheng, Z. Wu, S. Huyan, H.-C. Wu, Y. Nie, K. Cho, and C.-W. Chu, Higher superconducting transition temperature by breaking the universal pressure relation, Proc. Natl. Acad. Sci. (USA) **116**, 2004 (2019).

[21] Y. Zhou, J. Guo, S. Cai, J. Zhao, G. Gu, C. Lin, H. Yan, C. Huang, C. Yang, S. Long, Y. Gong, Y. Li, X. Li, Q. Wu, J. Hu, X. Zhou, T. Xiang, and L. Sun, Quantum phase transition from superconducting to insulating-like state in a pressurized cuprate superconductor, Nat. Phys. **18**, 406 (2022).

[22] R. Matsumoto, S. Yamamoto, Y. Takano, and H. Tanaka, Crystal growth and high-pressure effects of Bi-based superconducting whiskers, ACS Omega **6**, 12179 (2021).

[23] M. Hervieu, C. Michel, B. Domenges, Y. Laligant, A. Lebail, G. Ferey, and B. Raveau, Electron microscopy study of the superconductor $Bi_2Sr_2CaCu_2O_{8+\delta}$, Mod. Phys. Lett. B **02**, 491 (1988).

[24] V. F. Shamrai, Crystal structures and superconductivity of bismuth high temperature superconductors (Review), Inorg. Mater. Appl. Res. **4**, 273 (2013).

[25] E. V. Antipov and A. M. Abakumov, Structural design of superconductors based in complex copper oxides, Phys. Usp. **51**, 180 (2008).

[26] A. Nakayama, Y. Onda, S. Yamada, H. Fujihisa, M. Sakata, Y. Nakamoto, K. Shimizu, S. Nakano, A. Ohmura, F. Ishikawa, and Y. Yamada, Collapse of CuO double chains and suppression of superconductivity in high-pressure phase of $YBa_2Cu_4O_8$, J. Phys. Soc. Jpn. **83**, 093601 (2014).

[27] H. Ludwig, W. Fietz, M. Dietrich, H. Wuhl, J. Karpinski, E. Kaldis, and S. Rusiecki, X-ray investigations of $Y_1Ba_2Cu_4O_8$ under high pressure, Physica C **167**, 335 (1990).

[28] R. Nelmes, J. Loveday, E. Kaldis, and J. Karpinski, The crystal structure of $YBa_2Cu_4O_8$ as a function of pressure up to 5 GPa, Physica C **172**, 311 (1990).

[29] H. Takagi, R. J. Cava, M. Marezio, B. Batlogg, J. J. Krajewski, W. F. Peck, P. Bordet, and D. E. Cox, Disappearance of Superconductivity in Overdoped $La_{2-x}Sr_xCuO_4$ at a Structural Phase Boundary, Phys. Rev. Lett. **68**, 3777 (1992).

[30] C. Looney, J. S. Schilling, and Y. Shimakawa, The influence of pressure-induced relaxation effects on T_c in $TlS_2CaCu_2O_{7-\delta}$, Physica C **297**, 239 (1998).

[31] S. Sadewasser, J. S. Schilling, J. Wagner, O. Chmaissem, J. D. Jorgensen, D. G. Hinks, and B. Dabrowski, Relaxation effects in the transition temperature of superconducting $HgBa_2CuO_{4+\delta}$, Phys. Rev. B **60**, 9827 (1999).

[32] J. S. Olsen, S. Steenstrup, L. Gerward, and B. Sundqvist, High pressure studies up to 50 GPa of Bi-based high-T_c superconductors, Phys. Scr. **44**, 211 (1991).

[33] J.-R. Gavarri, O. Monnereau, G. Vacquier, C. Carel, and C. Vettier, Anisotropic compressibility of the orthorhombic phase $Bi_2Sr_2Ca_1Cu_2O_8$, Physica C **172**, 213 (1990).

[34] J.-B. Zhang, L.-Y. Tang, J. Zhang, Z.-X. Qin, X.-J. Zeng, J. Liu, W. Jin-Sheng, X. Zhi-Jun, G. Genda, and X.-J.

Chen, Pressure-induced isostructural phase transition in $Bi_2Sr_2CaCu_2O_{8+\delta}$, Chin. Phys. C **37**, 088003 (2013).

[35] J. Dominec, P. Vasek, V. Plechacek, and C. Laermans, Elastic moduli for three superconducting phases of Bi-Sr-Ca-Cu-O, Mod. Phys. Lett. B **06**, 1049 (1992).

[36] Y. Tajima, M. Hikita, M. Suzuki, and Y. Hidaka, Pressure-effect study on high-T_c superconducting single crystal of 84 K Bi-Sr-Ca-Cu-O system, Physica C **158**, 237 (1989).

[37] T. Yoneda, Y. Mori, Y. Akahama, M. Kobayashi, and H. Kawamura, Pressure-Effect Study on the High-T_c Superconductor Bi(Pb)-Sr-Ca-Cu-O System, Jpn. J. Appl. Phys. **29**, L1396 (1990).

[38] M. B. Solunke, K. B. Modi, V. K. Lakhani, K. B. Zankat, P. U. Sharma, P. V. Reddy, and S. S. Shah, Effect of Ag^+-addition on elastic behaviour of Bi-2212 superconductors, Ind. J. Pure Appl. Phys. **45**, 3 (2007).

[39] C. Fanggao, M. Cankurtaran, G. A. Saunders, A. Al-Kheffaji, D. P. Almond, and P. J. Ford, Ultrasonic evidence of low bulk modulus and large vibrational anharmonicity in the bismuth cuprate high $T_c$superconductors, Supercond. Sci. Technol. **4**, 13 (1991).

[40] R. Munro, *Elastic Moduli Data for Polycrystalline Ceramics*, tech. rep. NISTR 6853 (National Institute of Standards and Technology, Gaithersburg, MD, 2002).

[41] T. Seetawan, Synthesis of BSCCO Amorphous Materials by Melt-Quenched Method, Asia Pacific J. Sci. Tech. **13**, 731 (2008).

[42] M. Rivers, V. Prakapenka, A. Kubo, C. Pullins, C. Holl, and S. Jacobsen, The COMPRES/GSECARS gas-loading system for diamond anvil cells at the Advanced Photon Source, High Press. Res. **28**, 273 (2008).

[43] S. Klotz, J.-C. Chervin, P. Munsch, and G. Le Marchand, Hydrostatic limits of 11 pressure transmitting media, J. Phys. D **42**, 075413 (2009).

[44] R. Hrubiak, S. Sinogeikin, E. Rod, and G. Shen, The laser micro-machining system for diamond anvil cell experiments and general precision machining applications at the High Pressure Collaborative Access Team, Rev. Sci. Instrum. **86**, 072202 (2015).

[45] L. W. Finger, R. M. Hazen, G. Zou, H. K. Mao, and P. M. Bell, Structure and compression of crystalline argon and neon at high pressure and room temperature, Appl. Phys. Lett. **39**, 892 (1981).

[46] R. J. Hemley, C. S. Zha, A. P. Jephcoat, H. K. Mao, L. W. Finger, and D. E. Cox, X-ray diffraction and equation of state of solid neon to 110 GPa, Phys. Rev. B **39**, 11820 (1989).

[47] C. Park, D. Popov, D. Ikuta, C. Lin, C. Kenney-Benson, E. Rod, A. Bommannavar, and G. Shen, New developments in micro-X-ray diffraction and X-ray absorption spectroscopy for high-pressure research at 16-BM-D at the Advanced Photon Source, Rev. Sci. Instrum. **86**, 072205 (2015).

[48] O. L. Anderson, D. G. Isaak, and S. Yamamoto, Anharmonicity and the equation of state for gold, J. Appl. Phys. **65**, 1534 (1989).

[49] J. A. Xu, H. K. Mao, and P. M. Bell, High-Pressure Ruby and Diamond Fluorescence: Observations at 0.21 to 0.55 Terapascal, Science **232**, 1404 (1986).

[50] C. Prescher and V. B. Prakapenka, DIOPTAS: a program for reduction of two-dimensional X-ray diffraction data and data exploration, High Press. Res. **35**, 223 (2015).

[51] P. Vinet, J. R. Smith, J. Ferrante, and J. H. Rose, Temperature effects on the universal equation of state of solids, Phys. Rev. B **35**, 1945 (1987).

[52] See Supplemental Material at http://link.aps.org/supplemental/10.1103/PhysRevMaterials.7.064803 for additional graphs and tables.

[53] V. Petříček, M. Dušek, and L. Palatinus, Crystallographic Computing System JANA2006: General features, Z. Kristallogr.-Cryst. Mater. **229**, 345 (2014).

[54] D. Ariosa, H. Berger, T. Schmauder, D. Pavuna, G. Margaritondo, S. Christensen, R. J. Kelley, and M. Onellion, Periodic c-axis modulation and crystallographic Fourier analysis of $Bi_2Sr_2Ca_nCu_{n+1}O_{6+2n+x}$ (n=0,1) single crystals with excess Bi, Physica C **351**, 251 (2001).

[55] V. N. Timofeev and I. G. Gorlova, Growth defects in BSCCO (2212) single crystal whiskers, Physica C **309**, 113 (1998).

[56] H. W. Zandbergen, P. Groen, G. Van Tendeloo, J. Van Landuyt, and S. Amelinckx, Electron diffraction and electron microscopy of the high T_c superconductive phase in the Bi-Ca-Sr-Cu-O system, Solid State Commun. **66**, 397 (1988).

[57] N. Poccia, S. F. Zhao, H. Yoo, X. Huang, H. Yan, Y. S. Chu, R. Zhong, G. Gu, C. Mazzoli, K. Watanabe, T. Taniguchi, G. Campi, V. M. Vinokur, and P. Kim, Spatially correlated incommensurate lattice modulations in an atomically thin high-temperature $Bi_{2.1}Sr_{1.9}CaCu_{2.0}O_{8+y}$ superconductor, Phys. Rev. Mater. **4**, 114007 (2020).

[58] J. M. Tarascon, W. R. McKinnon, P. Barboux, D. M. Hwang, B. G. Bagley, L. H. Greene, G. W. Hull, Y. LePage, N. Stoffel, and M. Giroud, Preparation, structure, and properties of the superconducting compound series $Bi_2Sr_2Ca_{n-1}Cu_nO_y$ with $n = 1$, 2, and 3, Phys. Rev. B **38**, 8885 (1988).

[59] S. V. Pryanichnikov, S. G. Titova, Y. V. Zubavichus, A. A. Veligzhanin, A. M. Yankin, S. S. Agafonov, and E. V. Yakovenko, Nonmonotonic structural changes in HTSC Bi-2201 ceramics depending on oxygen nonstoichiometry, Phys. Met. Metallogr. **113**, 779 (2012).

[60] N. R. Khasanova and E. V. Antipov, Bi-2201 phases synthesis, structures and superconducting properties, Physica C **246**, 241 (1995).

[61] A. V. Mironov, V. Petříček, N. R. Khasanova, and E. V. Antipov, New insight on bismuth cuprates with incommensurate modulated structures, Acta Crystallogr. B **72**, 395 (2016).

[62] A. Pereira, D. Errandonea, A. Beltrán, L. Gracia, O. Gomis, J. Sans, B. Garcia-Domene, A. Miquel Veyrat, F. J. Manjon, A. Munoz, and C. Popescu, Structural study of α-Bi_2O_3 under pressure, J. Phys.: Condens. Matter **25**, 475402 (2013).

[63] D. A. Fredenburg and N. N. Thadhani, High-pressure equation of state properties of bismuth oxide, J. Appl. Phys. **110**, 063510 (2011).

[64] Y. Gao, P. Coppens, D. E. Cox, and A. R. Moodenbaugh, Combined X-ray single-crystal and neutron powder refinement of modulated structures and application to the incommensurately modulated structure of $Bi_2Sr_2CaCu_2O_{8+y}$, Acta Crystallogr. A **49**, 141 (1993).

[65] J. M. Tarascon, Y. Le Page, P. Barboux, B. G. Bagley, L. H. Greene, W. R. McKinnon, G. W. Hull, M. Giroud, and D. M. Hwang, Crystal substructure and physical properties of the superconducting phase $Bi_4SrCa_6Cu_4O_{16+x}$, Phys. Rev. B **37**, 9382 (1988).

[66] V. Petricek, Y. Gao, P. Lee, and P. Coppens, X-ray analysis of the incommensurate modulation in the 2:2:1:2 Bi-Sr-Ca-Cu-O superconductor including the oxygen atoms, Phys. Rev. B **42**, 387 (1990).

[67] L. Gao, Y. Y. Xue, F. Chen, Q. Xiong, R. L. Meng, D. Ramirez, C. W. Chu, J. H. Eggert, and H. K. Mao, Superconductivity up to 164 K in $HgBa_2Ca_{m-1}Cu_mO_{2m+2+\delta}$ (m=1, 2, and 3) under quasihydrostatic pressures, Phys. Rev. B **50**, 4260 (1994).

[68] J. S. Olsen, S. Steenstrup, I. Johannsen, and L. Gerward, High pressure studies of the high temperature superconductors $RBa_2Cu_3O_{9-\delta}$ with R: Y, Eu and Ho up to 60 GPa, Z. Phys. B **72**, 165 (1988).

[69] M. Babaei and D. K. Ross, A determination of the variation in the lattice parameters of $Bi_2Sr_2CaCu_2O_{8+x}$ (Bi-2212) as a function of temperature and oxygen content, Physica C **425**, 130 (2005).

[70] V. F. Shamray, A. B. Mikhailova, and A. V. Mitin, Crystal structure and superconductivity of Bi-2223, Crystallogr. Rep. **54**, 584 (2009).

[71] A. Maljuk and C. T. Lin, Floating Zone Growth of $Bi_2Sr_2Ca_2Cu_3O_y$ Superconductor, Crystals **6**, 62 (2016).

[72] E. Giannini, N. Clayton, N. Musolino, A. Piriou, R. Gladyshevskii, and R. Flukiger, Growth and superconducting properties of Pb-free and Pb-doped Bi-2223 crystals, IEEE Trans. Appl. Supercond. **15**, 3102 (2005).

[73] F. Birch, Finite Elastic Strain of Cubic Crystals, Phys. Rev. **71**, 809 (1947).

[74] W. C. Overton Jr., Relation between Ultrasonically Measured Properties and the Coefficients in the Solid Equation of State, J. Chem. Phys. **37**, 116 (1962).

[75] A. Al-Kheffaji, M. Cankurtaran, G. A. Saunders, D. P. Almond, E. F. Lambson, and R. C. J. Draper, Elastic behaviour under pressure of high-T_c superconductors $RBa_2Cu_3O_{7-x}$ (R = Y, Gd and Eu), Philos. Mag. B **59**, 487 (1989).

[76] M. Cankurtaran, G. A. Saunders, J. R. Willis, A. Al-Kheffaji, and D. P. Almond, Bulk modulus and its pressure derivative of $YB_2Cu_3O_{7-x}$, Phys. Rev. B **39**, 2872 (1989).

[77] H. Jin and J. Kötzler, Growth and superconductivity of La-doped Bi-2201 whiskers, Mater. Res. Bull. **35**, 1805 (2000).

[78] J. I. Gorina, G. A. Kaljuzhnaia, N. N. Sentjurina, and V. A. Stepanov, Dependence of superconducting properties of undoped Bi2201 single crystals on conditions of their free growth in gas-filled cavities of a molten salt, Solid State Commun. **126**, 557 (2003).

[79] W. Voigt, Ueber die Beziehung zwischen den beiden Elasticitätsconstanten isotroper Körper, Ann. Phys. **274**, 573 (1889).

[80] A. Reuss, Berechnung der Fliessgrenze von Mischkristallen auf Grund der Plastizitätsbedingung für Einkristalle., ZAMM **9**, 49 (1929).

[81] R. E. Cohen, O. Gülseren, and R. J. Hemley, Accuracy of equation-of-state formulations, Am. Mineral. **85**, 338 (2000).

[82] X. Yang, Q. Li, R. Liu, B. Liu, S. Jiang, K. Yang, J. Liu, Z. Chen, B. Zou, T. Cui, and B. Liu, A novel pressure-induced phase transition in $CaZrO_3$, CrystEngComm **16**, 4441 (2014).

[83] K. Niwa, T. Yagi, and K. Ohgushi, Elasticity of $CaIrO_3$ with perovskite and post-perovskite structure, Phys. Chem. Miner. **38**, 21 (2011).

[84] J. D. Jorgensen, S. Pei, P. Lightfoot, D. G. Hinks, B. W. Veal, B. Dabrowski, A. P. Paulikas, R. Kleb, and I. D. Brown, Pressure-induced charge transfer and dT_c/dP in $YBa_2Cu_3O_{7-x}$, Physica C **171**, 93 (1990).

[85] R. P. Gupta and M. Gupta, Relationship between pressure-induced charge transfer and the superconducting transition temperature in $YBa_2Cu_3O_{7-\delta}$ superconductors, Phys. Rev. B **51**, 11760 (1995).

[86] S. M. O'Mahony, W. Ren, W. Chen, Y. X. Chong, X. Liu, H. Eisaki, S. Uchida, M. H. Hamidian, and J. C. S. Davis, On the electron pairing mechanism of copper-oxide high temperature superconductivity, Proc. Natl. Acad. Sci. (USA) **119**, e2207449119 (2022).

[87] S. Speziale, C.-S. Zha, T. S. Duffy, R. J. Hemley, and H.-k. Mao, Quasi-hydrostatic compression of magnesium oxide to 52 GPa: Implications for the pressure-volume-temperature equation of state, J. Geophys. Res.: Solid Earth **106**, 515 (2001).

[88] P. Richet, H.-K. Mao, and P. M. Bell, Static compression and equation of state of CaO to 1.35 Mbar, J. Geophys. Res.: Solid Earth **93**, 15279 (1988).

[89] A. Dewaele, Equations of State of Simple Solids (Including Pb, NaCl and LiF) Compressed in Helium or Neon in the Mbar Range, Minerals **9**, 684 (2019).

[90] Z. P. Chang and E. K. Graham, Elastic properties of oxides in the NaCl-structure, J. Phys. Chem. Solids **38**, 1355 (1977).

[91] R. Jeanloz, Universal equation of state, Phys. Rev. B **38**, 805 (1988).

[92] R. J. Angel, Equations of state, in *High-Temperature and High-Pressure Crystal Chemistry*, edited by R. M. Hazen, R. T. Downs and P. H. Ribbe (Mineralogical Society of America, 2000), Vol. 41, pp. 35–59.

[93] T. J. B. Holland and R. Powell, An internally consistent thermodynamic data set for phases of petrological interest, J. Metamorph. Geol. **16**, 309 (1998).

[94] C. W. Chu, L. Gao, F. Chen, Z. J. Huang, R. L. Meng, and Y. Y. Xue, Superconductivity above 150 K in $HgBa_2Ca_2Cu_3O_{8+\delta}$ at high pressures, Nature **365**, 323 (1993).

[95] N. Takeshita, A. Yamamoto, A. Iyo, and H. Eisaki, Zero Resistivity above 150 K in $HgBa_2Ca_2Cu_3O_{8+\delta}$ at High Pressure, J. Phys. Soc. Jpn. **82**, 023711 (2013).

[96] M. Nuñez-Regueiro, J.-L. Tholence, E. V. Antipov, J.-J. Capponi, and M. Marezio, Pressure-Induced Enhancement of T_c Above 150 K in Hg-1223, Science **262**, 97 (1993).

[97] M. Monteverde, C. Acha, M. Núñez-Regueiro, D. A. Pavlov, K. A. Lokshin, S. N. Putilin, and E. V. Antipov, High-pressure effects in fluorinated $HgBa_2Ca_2Cu_3O_{8+\delta}$, Europhys. Lett. **72**, 458 (2005).

[98] A. Yamamoto, N. Takeshita, C. Terakura, and Y. Tokura, High pressure effects revisited for the cuprate superconductor family with highest critical temperature, Nat. Commun. **6**, 8990 (2015).

[99] D. T. Jover, R. J. Wijngaarden, H. Wilhelm, R. Griessen, S. M. Loureiro, J. Capponi, A. Schilling, and H. R. Ott, Pressure dependence of the superconducting critical temperature of $HgBa_2Ca_2Cu_3O_{8+y}$ and $HgBa_2Ca_3Cu_4O_{10+y}$ up to 30 GPa, Phys. Rev. B **54**, 4265 (1996).

[100] H. Ihara, M. Hirabayashi, H. Tanino, K. Tokiwa, H. Ozawa, Y. Akahama, and H. Kawamura, The Resistivity Measurements of $HgBa_2Ca_2Cu_3O_{8+x}$ and $HgBa_2Ca_3Cu_4O_{10+x}$ Superconduc-

tors under High Pressure, Jpn. J. Appl. Phys. **32**, L1732 (1993).

[101] D. P. Matheis and R. L. Snyder, The Crystal Structures and Powder Diffraction Patterns of the Bismuth and Thallium Ruddlesden-Popper Copper Oxide Superconductors, Powder Diffr. **5**, 8 (1990).

[102] R. Wesche, S. Kasap, and P. Capper, High-Temperature Superconductors, in *Springer Handbook of Electronic and Photonic Materials*, edited by S. Kasap and P. Capper (Springer International, Cham, 2017), p. 1–1.

[103] X.-J. Chen, V. V. Struzhkin, R. J. Hemley, H.-K. Mao, and C. Kendziora, High-pressure phase diagram of $Bi_2Sr_2CaCu_2O_{8+\delta}$ single crystals, Phys. Rev. B **70**, 214502 (2004).

[104] C.-S. Zha, H.-K. Mao, and R. J. Hemley, Elasticity of MgO and a primary pressure scale to 55 GPa, Proc. Natl. Acad. Sci. (USA) **97**, 13494 (2000).